Gastrointest Radiol 17:63–73 (1992)

Gastrointestinal Radiology

Contribution of CT to Characterization of Focal Nodular Hyperplasia of the Liver

Carlo Procacci,[1] Carlo Fugazzola,[1] Marco Cinquino,[1] Gerardo Mangiante,[2] Loretta Zonta,[1] Ivo Andrea Bergamo Andreis,[1] Nicola Nicoli,[2] and Gian Franco Pistolesi[1]

Departments of [1] Radiology and [2] Surgery, University Hospital, Verona, Italy

Abstract. Our personal series of 20 cases of focal nodular hyperplasia (FNH) of the liver is presented. All lesions were studied with computed tomography (CT), 16 of which with surgical control. Retrospective evaluation of the CT features of the identified FNH, along with those of five hepatocellular adenomas (HCA) and 30 hepatocellular carcinomas (HCC), allowed the definition of specific patterns leading to a correct characterization of FNH in 78% of cases. This greatly reduced the diagnostic errors, with the sole exception of patients with fatty liver in whom nuclear medicine may eventually provide a correct characterization. Fine-needle biopsy is thus only necessary in the dubious cases. A precise diagnostic workup of FNH is necessary, since it may avoid the surgical intervention.

Key words: Liver, benign lesions — Liver, focal nodular hyperplasia — Focal nodular hyperplasia, CT.

Focal nodular hyperplasia (FNH) is a pseudotumoral lesion of the liver, most often asymptomatic [1–6]. In the past FNH was usually an incidental finding at surgery or autopsy; its preoperative incidence has increased over the last years due to the easier identification by means of the new imaging modalities, notably ultrasonography (US) and computed tomography (CT).

The identification of this lesion does not unfortunately mean its proper characterization, since often problems of differential diagnosis arise vs. either benign or malignant liver tumors [7–10]. A proper characterization is nevertheless important due to the fact that, as for hemangiomas, surgery is not constantly required [3–6, 8, 11, 12]. Moreover, the need to clearly define radiologically this lesion is further justified by the difficulties met by fine-needle aspiration cytology in properly characterizing a FNH [3, 5, 6]. The aim of this paper is to report our personal experience on CT study of 20 FNH identified in 19 patients, in order to assess the reliability of this imaging modality for a proper characterization of the lesion.

Address offprint requests to: Carlo Procacci, M.D., Department of Radiology, University Hospital, I-37134 Verona, Italy

Materials and Methods

The personal experience refers to 20 FNH identified in 19 patients (one patient presented two lesions; two lesions were associated with an hemangioma): surgical control (either resection or wide wedge biopsy) was performed in 16 patients; the three remaining are being followed, respectively, 30, 45, and 64 months from the initial diagnosis.

The retrospective analysis of the FNH identified by CT was done blindly, adding five hepatocellular adenomas (HCA) and 30 hepatocellular carcinomas (HCC). The technique used for their evaluation is the same employed for the assessment of any solid liver mass: the preliminary unenhanced scan is followed by intravenous bolus injection of 30 ml of Conray 60% (Bracco Industria Chimica S.p.A., Milan, Italy) and then rapid drip infusion of 120 ml of the same contrast material. A third control, at the site of the lesion, is performed 5 min after terminating the drip infusion; in some circumstances, late scans (30–40 min) were also obtained.

Results

The results refer to the global series of 54 patients presenting respectively FNH (19 of 54), HCA (5 of 54), and HCC (30 of 54).

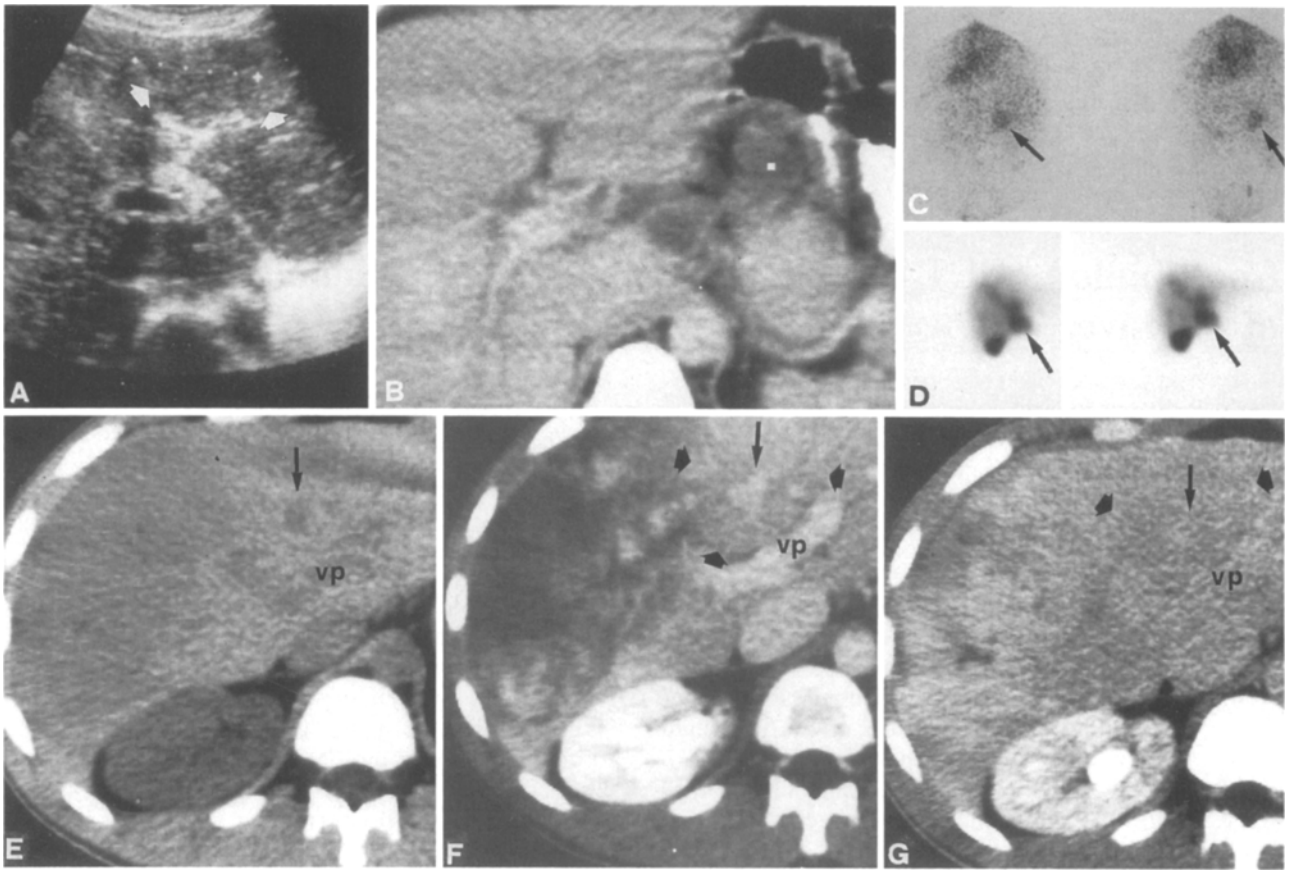

Fig. 1. *FNH: CT false negatives.* **A–D** *First case.* **A** US (axial scan) shows an ovoid mass (*arrows*), isoechoic vs. the adjacent normal parenchyma. **B** On the enhanced CT scan no abnormalities can be recognized within the left lobe. **C,D** The scintigraphic study shows increased uptake of the radionuclide within the mass (*arrows*), both on the 99mTc sulfur colloid **(C)** and on the 99mTc-HIDA **(D)** scans. **E–G** *Second case.* The CT study—both the unenhanced **(E)** and respectively the early **(F)** and late **(G)** enhanced scans—shows a large mass within the right liver lobe, with the features of an hemangioma. Only a retrospective evaluation, based on the surgical findings, allows recognition of the FNH (*short arrows*), with central scar (*long arrow*), located in front of the portal vein (*vp*).

Identification

Only the 20 FNH are referred to since the other tumors (HCA and HCC) (inserted in this series only in order to assess CT characterization capabilities) were constantly identified.

CT identified 18 of 20 FNH (90%), with two false-negatives (10%). In one false-negative case, the lesion, 5 cm in diameter and involving the left lobe, had been identified by US (Fig. 1A) and was confirmed (Fig. 1C and D) by nuclear medicine (NM). On the CT scan, also at a retrospective evaluation, the lesion could not be identified, being isodense vs. the normal parenchyma through all the phases of the examination (Fig. 1B). In the other false-negative case, the tumor, located adjacent to a large hemangioma, was identified only retrospectively (Fig. 1E–G) following the topographic guidelines provided by the surgeon. The mass was in fact isodense in all phases of the exam, however, with a central hypodense scar—the only feature useful for a proper identification.

Characterization

We refer to the global series of 54 patients, with exception of the two missed FNH, namely 53 masses, keeping benign and malignant lesions separated (Table 1).

Benign lesions. The *diagnosis of benign lesions* was achieved in 83% (19 of 23) of the identified benign masses (18 FNH and 5 HCA), notably in 94% of FNH (17 of 18) and 40% of HCA (2 of 5).

The *proper lesion characterization* was reached in 65% (15 of 23) of cases (i.e., in 14 of 18 FNH and 1 of 5 HCA).

As to FNH its characterization could be achieved on the basis of the following features (Table 2).

Table 1. Analysis of the CT results relating to the characterization of identified lesions

Lesion	No. of cases	Diagnosis of		Characterization			Nonspecific diagnosis		Wrong diagnosis	
		Benign lesion	Malignant lesion	FNH	HCA	HCC	Benign lesion	Malignant lesion	FNH	HCC
FNH	18	17/18 (94%)	—	14/18 (78%)	—	—	3/18 (16%)	—	—	1/18 (6%)
HCA	5	2/5 (40%)	—	—	1/5 (20%)	—	—	—	1/5 (20%)	3/5 (60%)
Benign lesions (FNH + HCA)	23	19/23 (83%)	—	15/23 (65%)		—	3/23 (13%)	—	1/23 (4%)	4/23 (18%)
HCC	30	—	28/30 (93%)	—	—	9/30 (30%)	—	19/30 (63%)	2/30 (7%)	—

Table 2. CT features in the 18 identified FNH, and final diagnosis

Cases	∅ cm	Tumor density vs. normal parenchyma			Scar	Septa	Capsule	Vessel indentation	Opacif. biliary ductules	Final diagnosis
		Unenhanced	Early enhanced	Late enhanced						
1	5	<	=	=	−	−	+	−	−	FNH
2	5	<	=	=	−	+	−	−	−	FNH
3	4	<	=	=	+	−	−	−	−	FNH
4	5	<	=	=	+	+	+	+	−	FNH
5[a]	6	<	=	=	−	−	+	−	−	FNH
6[a]	3	<	=	=	−	−	+	−	−	FNH
7	4	=	=	=	+	−	−	−	−	FNH
8	6	=	=	=	+	−	−	−	−	FNH
9	4	=	=	=	−	−	−	+	−	FNH
10	6	<	=	=	−	−	−	−	−	FNH
11	9	=	=	=	−	+	+	+	+	FNH
12	5	<	=	=	+	−	−	−	−	FNH
13	6	<	=	=	+	−	−	−	−	FNH
14	2	=	=	=	−	−	−	−	−	FNH
15	7	<	<	<	−	−	−	−	−	HCC
16	3.5	=	>	>	−	−	−	−	−	Benign tumor
17	5	>	>	>	−	−	−	+	−	Benign tumor
18	4	=	>	>	−	−	−	−	−	Benign tumor
Total		(a)	(b)	(c)	6	3	5	4	1	—

< hypodense; = isodense; > hyperdense.
(a): < (10); = (7); > (1); (b): < (1); = (14); > (3); (c): < (1); = (14); > (3).
[a] Observed in the same patient.

Its *densitometric behavior,* both on the unenhanced and enhanced scans, was the conclusive sign for diagnosis. On the precontrast scan the mass was hypodense (Figs. 2A, D and G and 3A and E) in 9 of 14 cases and isodense (Fig. 4A) in 5 of 14; in postcontrast scans, both at the early and late controls, the lesion was constantly isodense vs. normal liver parenchyma (Figs. 2B, C, E, F, H, I; 3B, C, F–H; and 4B, C).

The *central scar* was present in 6 of 14 cases, and was hypodense in all on the unenhanced scan (Fig. 2A and D); in two cases it remained hypodense (Fig. 2E and F) and in four hyperdense (Fig. 2C) both at the early and late postcontrast scans (Fig. 2C).

The *fibrous septa* were detected only in 3 of 14 cases. The septa were thick, and were recognized both on the unenhanced (hypodense) and enhanced (hyperdense) scans. Their densitometric features, notably on the enhanced scans, were superimposable to those of scars (Fig. 3A–C). In no cases could persistent hypodensity of the septa be detected. In several lesions small endotumoral structures were

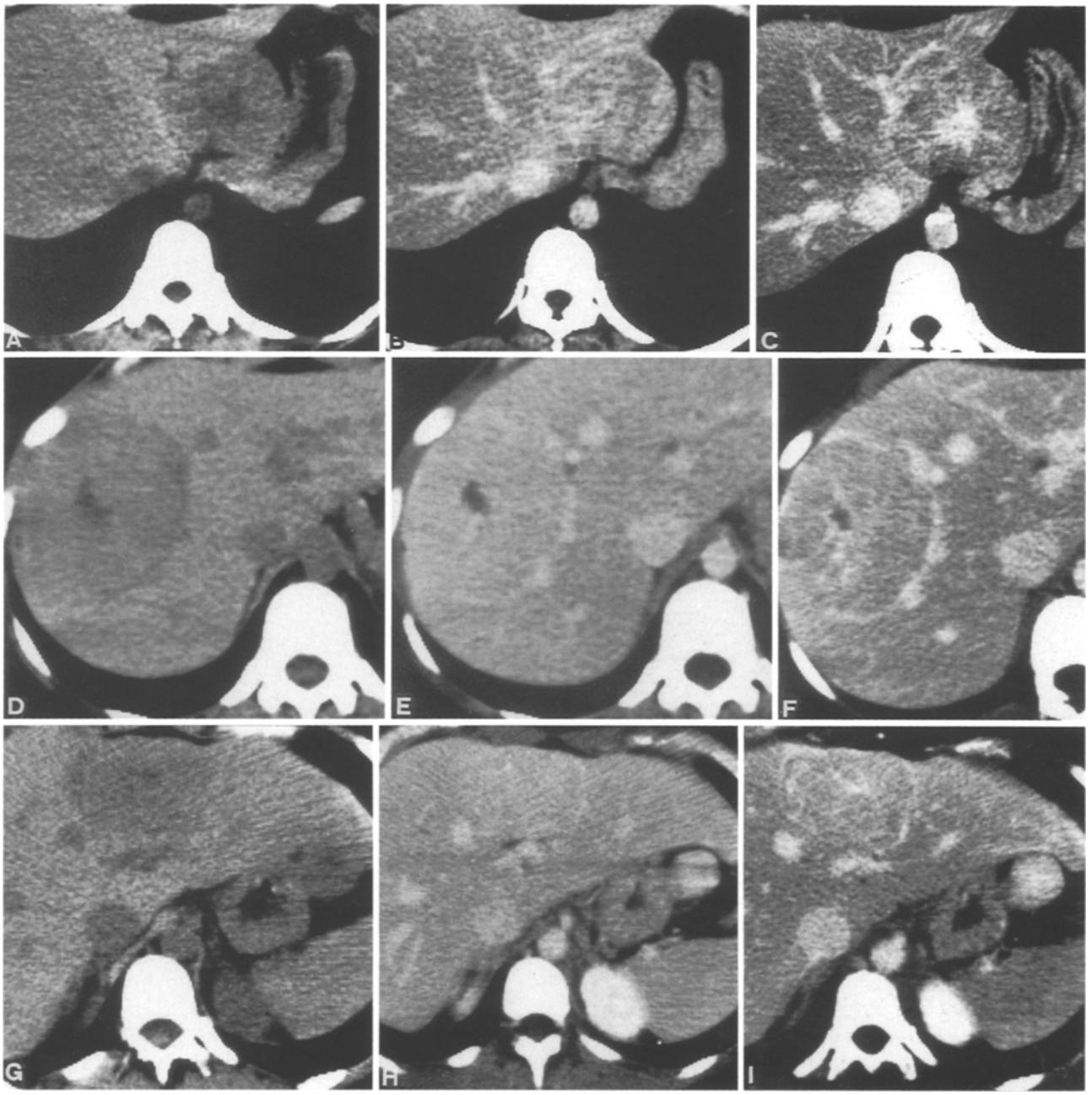

Fig. 2. *FNH: CT features.* **A–C** In the left liver lobe the lesion, hypodense with a central scar on the unenhanced scan, turns isodense on the enhanced scan (early and late phase); at the late phase the scar is hyperdense. **D–F** In the right lobe the mass is hypodense on the unenhanced scan, with a central scar and well-defined margins. The mass turns isodense on the enhanced scan with a hyperdense capsule; the central scar remains hypodense also on the late controls. **G–I** In the quadrate lobe the lesion, hypodense on the unenhanced scan with thin low-density septa, turns isodense on the enhanced scan; the late control shows a thin capsule and central septa, both hyperdense.

present, with attenuation values similar to those of septa; however, their vascular or fibrous origin was difficult to assess (Figs. 2G–I and 3E–H).

A *hyperdense rim* was demonstrated in 5 of 14 lesions on the enhanced scan, notably at the late control (Figs. 2F and 3B, C, G, H). In one case (Fig. 3A–C), FNH, besides presenting gross central fibrous septa, had a thick capsule, appearing hypodense on the unenhanced scan.

The *indentation on adjacent vascular structures,* notably the hepatic veins, played a basic role for the identification of a FNH (isodense vs. the adjacent normal parenchyma in all phases of the CT study) (Fig. 4).

The *opacification of the intratumoral biliary ductules,* by means of cholangiographic contrast material, was shown in one case (Fig. 3D).

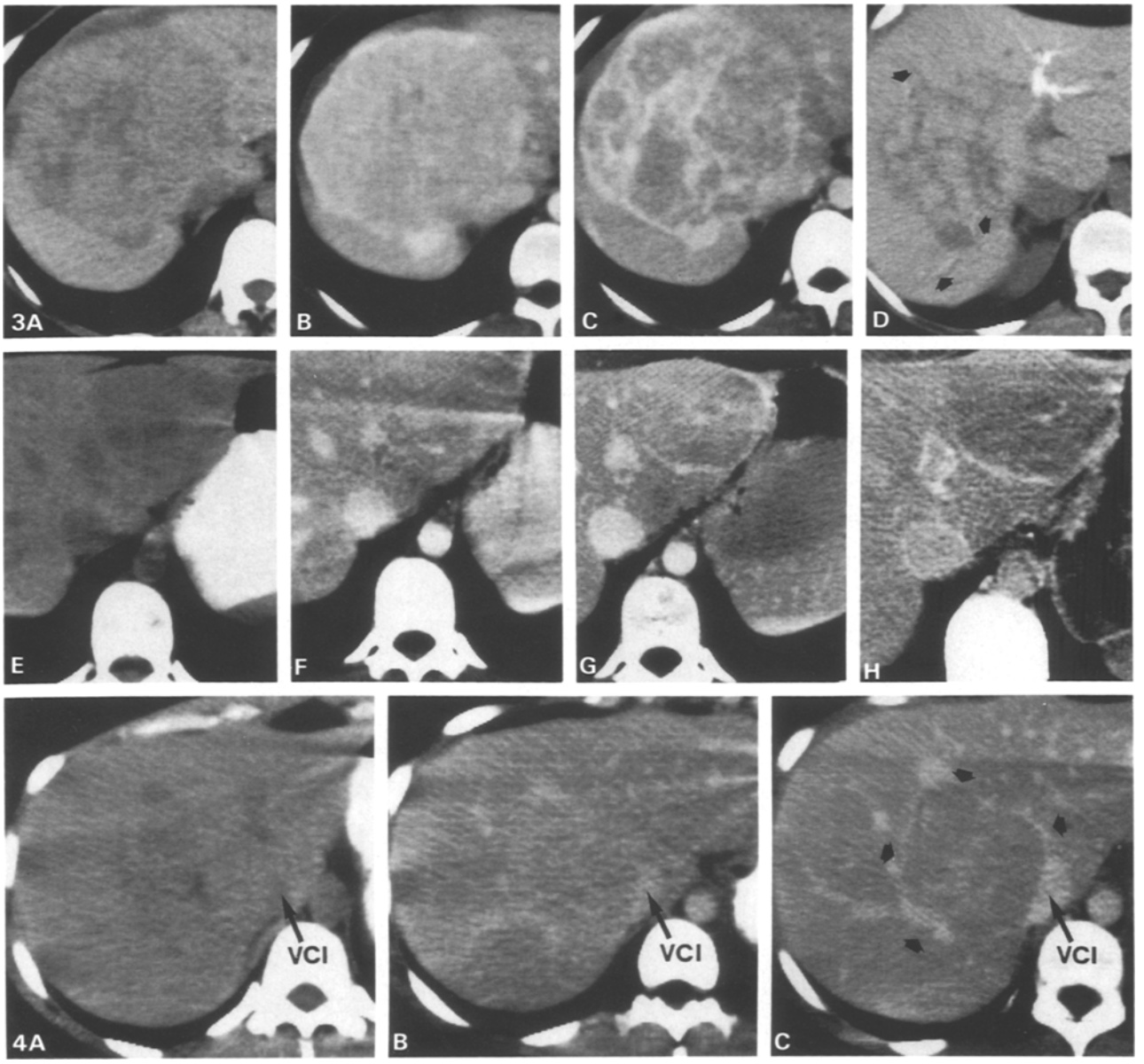

Fig. 3. *FNH: CT features.* **A–D** The right liver lobe is occupied by a large mass which, on the unenhanced scan **(A)**, is hypodense with septa and thick margin. On the enhanced scans **(B,C)** the lesion turns isodense, with hyperdense septa and capsule. The control, after drip infusion of cholangiographic contrast material **(D)**, shows the presence of hyperdense biliary ductules (*arrows*) within the lesion. **E–H** The left lobe is occupied by a large mass, hypodense on the unenhanced scan **(E)**. On the enhanced scans the lesion is isodense both at an early phase **(F)** and at later controls (5 min, **G**; 40 min, **H**); hyperdense capsule and central septa can be recognized.

Fig. 4. *FNH: CT features.* The lesion, constantly isodense vs. the adjacent parenchyma, is only identified at a late (5 min) enhanced scan, thanks to the indentation (*arrows*) on both the intrahepatic vessels and on the inferior vena cava (*VCI*).

The proper characterization of HCA could be assumed in only one case, which presented with acute abdominal pain and blood loss, due to the identification of hemorrhage within a lesion of the right liver lobe along with a large perihepatic blood collection due to rupture of the tumor (Fig. 6A).

The *nonspecific diagnosis* of a benign lesion was made in 3 of 23 (13%) cases, all FNH (Table 1). Such a diagnosis was made since the tumor was located in a fatty liver (Fig. 5), which made it impossible to confirm the usual density relation between mass and normal parenchyma.

The *wrong diagnosis* affected four HCA and one FNH (Table 1). One HCA was diagnosed a FNH since the tumor presented the same attenuation

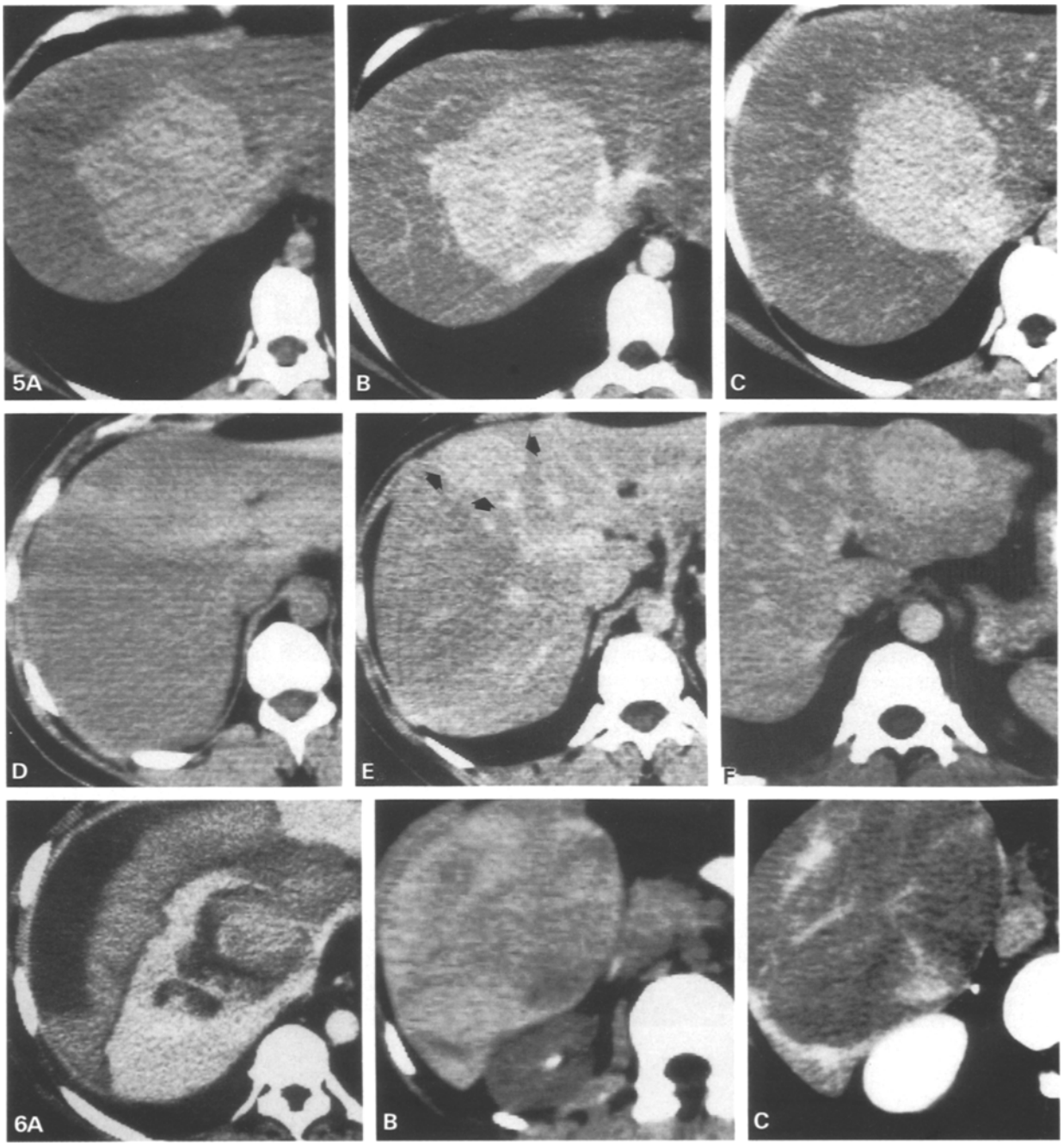

Fig. 5. *FNH: Nonspecific CT diagnoses.* **A–C** Within a fatty liver an evenly hyperdense lesion is recognized, both on the unenhanced **(A)** and enhanced **(B,C)** study. Indentation on the hepatic veins, as well as on the inferior vena cava. **D,E** The mass (*arrows*) can be recognized only on the enhanced scan (early phase), appearing hyperdense vs. the fatty liver. **F** A large hyperdense mass on the enhanced scan bulges from the anterior contour of the left lobe; diffuse fatty liver.

Fig. 6. *HCA: CT features.* **A** A large mass can be recognized within the right lobe, close to the diaphragm, presenting a large central area of hemorrhage and a notable perihepatic hematoma: CT diagnosis of HCA. **B,C** The tumor is isodense vs. the adjacent normal parenchyma both on the unenhanced **(B)** and enhanced **(C)** scans; central hyperdense septa: CT diagnosis of FNH.

values as a FNH, both on the unenhanced and enhanced scans (Fig. 6B and C). In the remaining 18% of cases (4 of 23) the wrong diagnosis was caused by the inhomogeneous pattern of the lesion, due to the presence of central hypodense areas, similar to those met in malignant tumors (Fig. 7): this feature was due, in FNH, to a coexisting hemangiomatous area within the mass (Fig. 7A and B); in HCA it was

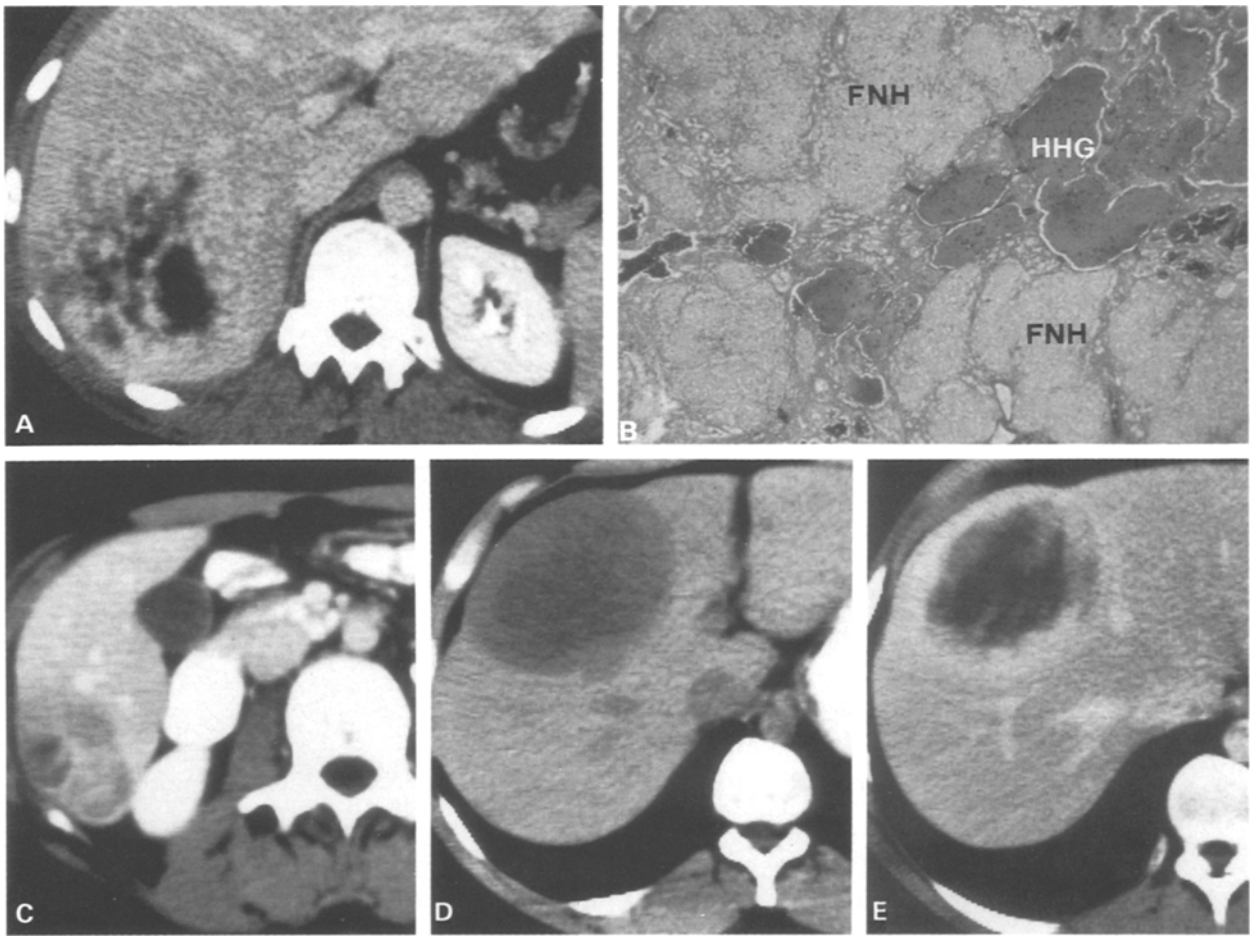

Fig. 7. *FNH and HCA: Incorrect CT diagnosis of malignancy.* **A,B** FNH: The lesion, on the enhanced scan, shows gross hypodense areas surrounded by parenchymal chunks presenting a density superimposable to that of the normal adjacent parenchyma. The following histologic examination (hematoxylin & eosin, ×100) shows the presence of hemangiomatous foci (HHG) surrounded by areas of FNH. **C** HCA: The tumor is hypodense and inhomogeneous due to a previous hemorrhage. **D,E** HCA: The tumor, both on the unenhanced and enhanced scans, is characterized by a thick peripheral rim and a large central hypodense area; in this case, the histologic control showed the presence of a large necrotic area.

caused by either a previous hemorrhage (Fig. 7C) or necrosis (Fig. 7D and E).

Malignant tumors. The *diagnosis of malignant tumors* was achieved in 93% (Table 1) of malignant lesions (28 of 30).

The *proper tumor characterization* (HCC) was hypothesized in only 30% of cases (9 of 30), all involving patients with liver cirrhosis; the lesions, fairly small in size, were characterized by homogeneous and persistent hypodensity vs. the adjacent parenchyma (the difference in attenuation value, on the postcontrast scan, was not superior, in these cases, to 20–30 HU). In this group a peripheral hyperdense capsule was constantly identified.

The *nonspecific diagnosis* of malignant tumor was on the contrary achieved in 63% of cases (19 of 30). The diagnosis had to be nonspecific, since the CT features were superimposable to those of other malignant neoplasms (cholangiocarcinoma, metastasis).

A *wrong diagnosis* of FNH was made in 7% of malignant tumors (2 of 30). In one case (fibrolamellar carcinoma) the error was caused by the detection of a central scar, respectively, hypodense on the unenhanced and hyperdense on the enhanced scans; in this tumor the constant, albeit slight, hypodensity vs. the normal liver parenchyma was not adequately assessed (Fig. 8A–C). In the other case, on the contrary, the lesion, slightly hypodense on the unenhanced scan, turned isodense in both the early and late enhanced scans, presenting an uncertain feature of thick capsule; in this mass the postcontrast isodensity of the tumor was due to the lesser attenuation values of the normal liver parenchyma, due to its steatosis (Fig. 8D and E).

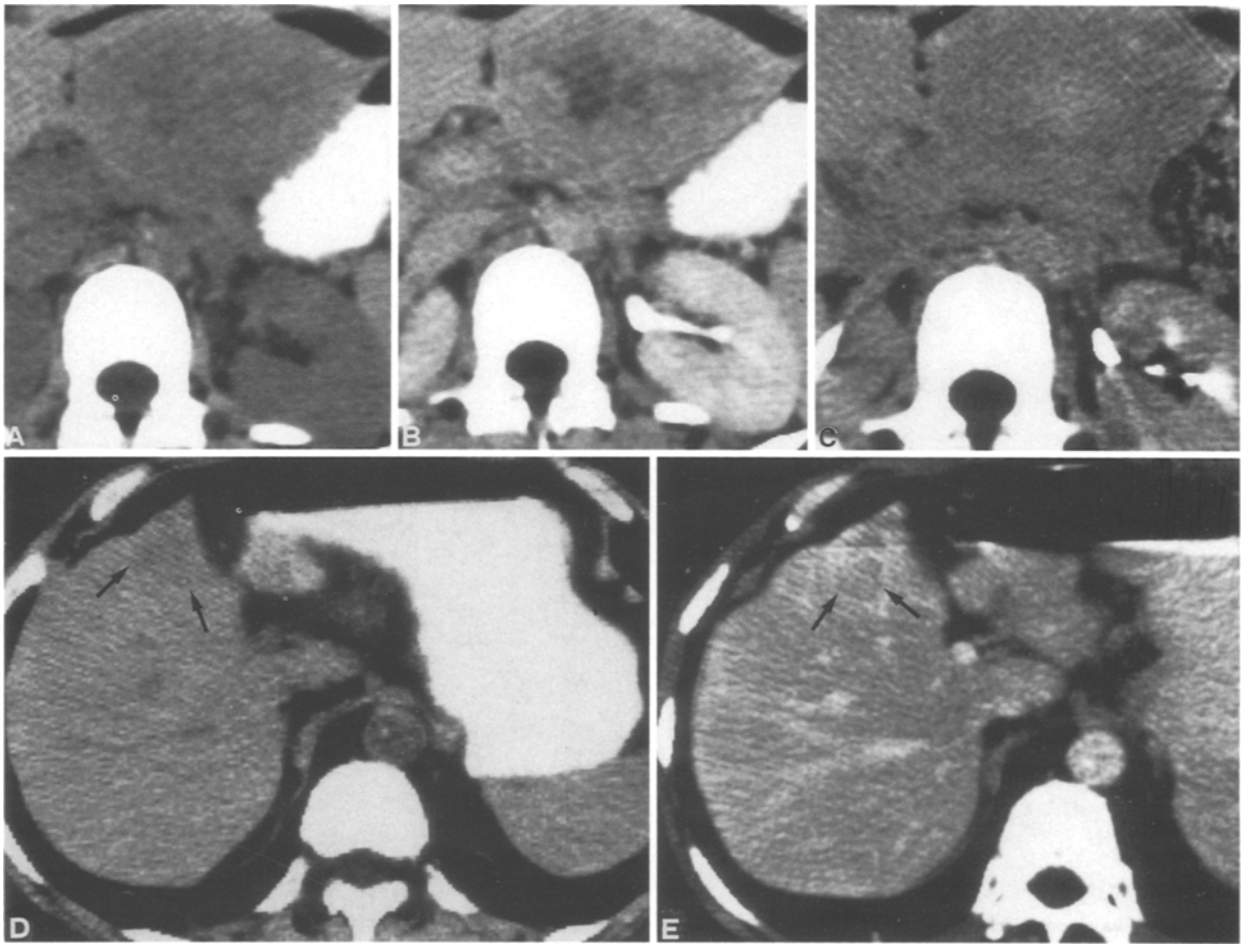

Fig. 8. *HCC: Incorrect CT diagnosis of FNH.* **A–C** Fibrolamellar carcinoma: The tumor, involving the left liver lobe, is slightly hypodense vs. the adjacent parenchyma, with a large central scar turning hyperdense on the late control. **D,E** HCC: The tumor (*arrows*), within a fairly fatty liver, is hypodense on the unenhanced scan and isodense after contrast materials administration.

Global Results

The *global results*, as to FNH, can be summarized as follows.

The *sensitivity* has to be differentiated according to the nonspecific diagnosis of benign lesion or to the specific diagnosis of FNH. In the first circumstance it reaches 85% (17 of 20), being possible also to consider those tumors which (due to the presence of liver steatosis) were not properly characterized; in the second event the sensitivity is lower, namely 70% (14 of 20).

The *specificity* is much higher, namely 91.5% (32 of 35). On this matter, one has to emphasize that the wrong diagnosis regarding the HCA (Fig. 6B and C) could not be corrected even retrospectively; on the contrary, a more thorough evaluation of the fibrolamellar carcinoma would have allowed a correct diagnosis (Fig. 8A–C), whereas in the other circumstance steatosis (Fig. 8D and E) should have led to a nonspecific diagnosis.

Discussion

The preoperative identification of FNH has become more frequent over the last years due to the availability of new imaging modalities, notably US and CT [2–5, 7, 11, 12].

A correct characterization of the lesion is useful, since it may avoid surgery; however, it is a goal difficult to reach.

Fine-needle *aspiration cytology* allows differentiation between FNH on the one hand and HCA and well-differentiated HCC on the other hand, based upon the identification of bile duct cells [13] which are not present in the latter; for the same reason it is not possible to differentiate between FNH and nor-

mal liver parenchyma [3, 6, 14]. This differential diagnosis can be achieved provided sufficient tissue (core biopsy) is obtained to allow a histologic diagnosis due to the peculiar architecture of FNH.

The *sonographic pattern* of FNH is most often nonspecific, indistinguishable from that of other liver masses, both benign and malignant [7, 12, 15].

The experience gained in the evaluation of FNH by means of *magnetic resonance* is still too limited to allow a final judgment on its reliability, as well as on the role it may play in the assessment of this pathology [6, 10, 16].

The accuracy of *nuclear medicine techniques* in the characterization of FNH is high, especially associating 99mTc sulfur colloid and HIDA scintigraphy [10, 12, 15–20]. FNH, characterized by a normal rate of functioning Kupffer cells [2–4], shows an homogeneous, normal or increased, uptake of 99mTc sulfur colloid and 99mTc-HIDA with delayed washout of the latter [17, 18]. By associating the two modalities, FNH can be differentiated from HCC and HCA. In HCC the uptake of 99mTc sulfur colloid or, more rarely, of 99mTc-HIDA is constantly inhomogeneous [19, 21–23]. In HCA, on the contrary, one may have an homogeneous uptake of 99mTc sulfur colloid [24], the uptake of 99mTc-HIDA being inhomogeneous and constantly characterized by fast wash-out [25].

Immediate resort to nuclear medicine after sonographic identification is however not justified, since FNH is a rarer lesion if compared with hemangiomas and malignant tumors, which do require a preliminary analysis by CT, this modality being both able to characterize them [26–28] and to provide, in the case of malignancy, also a judgment of resectability. Only the cases with a dubious CT diagnosis should then be submitted for nuclear medicine along with the rare, already correctly characterized benign lesions (FNH or HCA) for a further diagnostic confirmation. The data in the literature on the reliability of CT in the diagnosis of FNH are limited and often not comparable due to the different modalities of contrast material administration [7, 12, 16].

In our personal experience the CT sensitivity, resorting to the above mentioned technique, reaches 70% (14 of 20 cases) with an even higher specificity (91.5%). By excluding the false-negatives (2 of 20), as well as the FNH associated with liver steatosis (3 of 20), a proper characterization was almost constantly achieved (14 of 15) with one error of overevaluation (diagnosis of HCC).

The CT features which in our personal experience contributed to the diagnosis of FNH can be summarized as follows.

Attenuation value of the lesion. The mass appears either hypodense or isodense vs. the normal parenchyma on the unenhanced scan; in all cases it turns isodense both in the early and late controls after fast contrast material drip infusion.

The bolus technique achieves, in the early arterial phase, transient and intense hyperdensity of the mass [7]. This pattern, very useful for the identification of FNH isodense on the unenhanced scan, is nonspecific since HCC also presents the same feature [27, 28].

The isodensity of the lesion on the enhanced scan plays a basic role for a correct diagnosis; similar behavior has in fact been detected in only one case of HCA (Fig. 4B and C). As to the errors of underevaluation among HCC, fibrolamellar carcinoma has constantly been hypodense in the various phases of the study; however, the central scar has been wrongly given a basic diagnostic role. In the second case, the associated liver steatosis (the cause of isodensity of an otherwise hypodense lesion) was not considered.

Thus, only steatosis is a severe obstacle to the proper characterization of liver masses, since it cancels the value of the basic sign, namely the comparison between the density of the tumor and the adjacent normal parenchyma both on the unenhanced and enhanced scans [27, 29].

Central scar. This feature, once considered pathognomonic of FNH [3, 4, 6, 19, 30], provides on the contrary a fairly modest contribution to the characterization of the lesion, since it could be identified in only 46% of our cases. Moreover, the same feature can be detected in other tumors, notably fibrolamellar carcinoma [9, 10, 31–35]. The scar is constantly hypodense on the unenhanced scan, being most often hyperdense on the enhanced scan; in some instances it may nevertheless remain hypodense also on the late controls.

Capsule and fibrous septa. FNH is most often not properly separated from the normal parenchyma, being without capsule [3, 5, 6, 15, 19, 30]. If present, the capsule is very thin, being recognized only on the enhanced scan as a very tiny hyperdense rim.

The fibrous septa are always detected on the precontrast scan as hypodense bands, turning hyperdense on the postcontrast control.

Opacification of biliary ductules. The demonstration of biliary ductules within the fibrous septa by means of cholangiographic contrast material administration with consequent CT control is certainly a basic factor for the diagnosis of FNH [7, 36]; in our experience biliary ducts were opacified in only one of five cases.

Indentation on vascular structures. This feature plays an important role whenever the lesion is isodense vs. the normal parenchyma throughout the CT study, devoid of central scar, fibrous septa, or peripheral hyperdense rim.

The indentation on vascular structures can however be demonstrated only if the tumor is more than 3 cm in diameter.

Conclusions

Ultrasonography is usually able to identify a FNH. CT is a very useful imaging modality for the characterization of FNH, provided more controls are done during the exam; the only exception are patients with liver steatosis. In the cases with dubious CT features it is mandatory to resort to nuclear medicine, which is not hampered by the diagnostic problems met by CT. The impossibility to properly characterize the lesion makes it necessary to resort to needle biopsy, with the aim of acquiring a histologic diagnosis.

References

1. Edmonson HA. Tumors of the liver and intrahepatic bile ducts. In: *Atlas of tumors. Pathology section.* Washington, D.C.: AFIP, 1958:25
2. Ishak KG, Rabin L. Benign tumors of the liver. *Med Clin North Am* 1975;59:995–1013
3. Kerlin P, Davis GL, McGill DB, Weiland LH, Adson MA, Sheedy PF II. Hepatic adenoma and focal nodular hyperplasia: clinical, pathologic and radiologic features. *Gastroenterology* 1983;84:994–1002
4. Knowles DM, Casarella WJ, Johnson PM, Wolff M. The clinical, radiologic and pathologic characterization of benign hepatic neoplasm. Alleged association with oral contraceptives. *Medicine* 1978;57:223–237
5. Mangiante G, Pistacchi E, Marchiori L, Nicoli N, Dagradi A. Hepatocellular adenoma and focal nodular hyperplasia. *Chir Ital* 1989;41:117–128
6. Nichols FC, Van Heerden JA, Weiland LH. Benign liver tumors. *Surg Clin North Am* 1989;69:297–314
7. Mathieu D, Bruneton JN, Drouillard J, Pointreau CC, Vasile N. Hepatic adenoma and focal nodular hyperplasia: dynamic CT study. *Radiology* 1986;160:53–58
8. Nokes SR, Baker ME, Spritzer CE, Meyers W, Herfkens RJ. Hepatic adenoma: MR appearance mimicking focal nodular hyperplasia. *JCAT* 1988;12:885–887
9. Rummeny E, Weissleder R, Sironi S, Stark DD, Compton CC, Hahn PF, Saini S, Wittenberg J, Ferrucci JT. Central scar in primary liver tumors: MR features, specificity and pathologic correlation. *Radiology* 1989;171:323–326
10. Titelbaum DS, Burke DR, Meranze SG, Saul SH. Fibrolamellar hepatocellular carcinoma: pitfalls in nonoperative diagnosis. *Radiology* 1988;167:25–30
11. Huguet C, Nordlinger B, Baron JC, Parc R, Tubiana JM, Loygue J. Kystes congenitaux et tumeurs benignes du foie de l'adulte. Quelles indications chirurgicales? A propos de quarante-sept cas. *Ann Chir* 1986;40:231–235
12. Rogers JV, Mack LA, Freeny PC, Johnson ML, Sones PJ. Hepatic focal nodular hyperplasia: angiography, CT, sonography, and scintigraphy. *AJR* 1987;137:983–990
13. Ruschenburg I, Droese M. Fine needle aspiration cytology of focal nodular hyperplasia of the liver. *Acta Cytol* 1989;33:857–860
14. Klatskin J. Hepatic tumors: possible relationship to use of oral contraceptives. *Gastroenterology* 1977;73:386–394
15. D'Souza VJ, Sumner TE, Watson NE, Formanek AG. Focal nodular hyperplasia of the liver imaging by differing modalities. *Pediatr Radiol* 1983;13:77–81
16. Freeny PC. Radiologic diagnosis of hepatic neoplasms. *Postgrad Radiol* 1990;10:263–283
17. Biersak HJ, Thelen M, Torres JF, Lackner K, Winkler CG. Focal nodular hyperplasia of the liver as established by Tc 99m sulfur colloid and HIDA scintigraphy. *Radiology* 1980;137:187–190
18. Marabini A, Giorgetti PG, Zamboni M, Cavaggioni M, Braggio P, Nicoli N, Mangiante G. Nuclear medicine identification of hepatic focal nodular hyperplasia: experience of 10 cases. *J Nucl Med Allied Sci* 1989;33:154
19. Ros PR, Li KCP. Radiology of malignant and benign liver tumors. Part II: benign liver tumors. *Curr Probl Diagn Radiol* 1989;18:125–155
20. Welch TJ, Sheedy PF, Johnson CM, Stephens DH, Charboneau JW, Brown ML, May GR, Adson MA, McGill DB. Focal nodular hyperplasia and hepatic adenoma: comparison of angiography, CT, US, and scintigraphy. *Radiology* 1985;156:593–595
21. Calvet X, Pons F, Bruix J, Bru C, Lomena F, Herranz R, Brugera M, Faus R, Rodes J. Technetium-99m DISIDA hepatobiliary agent in diagnosis of hepatocellular carcinoma: relationship between detectability and tumor differentiation. *J Nucl Med* 1988; 29:1916–1920
22. Drane WE, Krasicky GA, Johnson DA. Radionuclide imaging of primary tumors and tumor-like conditions of the liver. *Clin Nucl Med* 1987;12:569–582
23. Savitch I, Kew MC, Paterson A, Esser JD, Levin J. Uptake of Tc-99m-Di-isopropyliminodiacetic acid by hepatocellular carcinoma: concise communication. *J Nucl Med* 1983;24:1119–1122
24. Lubbers PR, Ros PR, Goodman ZD, Ishak KG. Accumulation of technetium-99m sulfur colloid by hepatocellular adenoma: scintigraphic–pathologic correlation. *AJR* 1987;148:1105–1108
25. Vincent LM, Rho TH, McCartney WH, Mauro MA. Hepatic adenoma. Demonstration of discordant uptake with Tc-99m sulfur colloid and Tc-99m DISIDA. *Clin Nucl Med* 1984;9:415–416
26. Freeny PC, Marks WM. Hepatic hemangioma: dynamic bolus CT. *AJR* 1986;147:711–719
27. Freeny PC, Marks WM. Patterns of contrast enhancement of benign and malignant hepatic neoplasms during bolus dynamic and delayed CT. *Radiology* 1986;160:613–618
28. Itai Y, Ohtomo K, Kokubo T, Yamauchi T, Minami M, Yashiro N, Araki T. CT of hepatic masses: significance of prolonged and delayed enhancement. *AJR* 1986;146:729–733
29. Lewis E, Bernardino ME, Barnes PA, Parvey HR, Soo CS, Chuang VP. The fatty liver: pitfalls in the CT and angiographic evaluation of metastatic disease. *JCAT* 1983;7:235–241
30. Casarella WJ, Knowles DM, Wolff M, Johnson PM. Focal nodular hyperplasia and liver cell adenoma: radiologic and pathologic differentiation. *AJR* 1978;131:393–402
31. Bedi DG, Kumar R, Morettin LB, Gourley K. Fibrolamellar carcinoma of the liver: CT, ultrasound and angiography. *Europ J Radiol* 1988;8:109–112
32. Brandt DJ, Johnson CD, Stephens DH, Weiland LH. Imaging of fibrolamellar hepatocellular carcinoma. *AJR* 1988;151:295–299

33. Kane RA, Curatolo P, Khettry U. "Scar sign" on computed tomography and sonography in fibrolamellar hepatocellular carcinoma. *J Comput Tomogr* 1987;11:27–30
34. Saul SH, Titelbaum DS, Gansler TS, Varello M, Burke DR, Atkinson BF, Rosato EF. The fibrolamellar variant of hepatocellular carcinoma. Its association with focal nodular hyperplasia. *Cancer* 1987;60:3049–3055
35. Schiebler ML. Hepatocellular carcinoma: MR appearance mimicking focal nodular hyperplasia. *AJR* 1988;150:472
36. Huebener KH, Treught H. Administration of biliary contrast media in computed tomography. In: Felix R, et al., eds. *Contrast media in computed tomography. Proceedings of the international workshop, Berlin 1981*. Amsterdam: Excerpta Medica, 1981:46–51

Received: April 15, 1991; accepted: May 24, 1991